Talanta 89 (2012) 496–504

Contents lists available at SciVerse ScienceDirect

Talanta

journal homepage: www.elsevier.com/locate/talanta

Direct recognition and quantification by voltammetry of thiol/thioamide mixes in seawater

Luis M. Laglera [a,*], Antonio Tovar-Sánchez [b]

[a] Department of Chemistry, University of the Balearic Islands (UIB), Ctra Valldemossa km 7,5, Palma de Mallorca, Islas Baleares, 07122, Spain
[b] Department of Global Change Research, IMEDEA (CSIC-UIB), C/Miquel Marques, 21, Esporles, Islas Baleares, 07190, Spain

ARTICLE INFO

Article history:
Received 1 December 2011
Received in revised form
26 December 2011
Accepted 28 December 2011
Available online 3 January 2012

Keywords:
Thiols
Thioamides
Voltammetry
Seawater
Exudates
Pore waters

ABSTRACT

Thiols and thioamides form part of the pool of reduced sulfur substances (RSS) that modify the health of aquatic ecosystems acting as radical scavengers and heavy metal ligands. Their concentrations could be easily determined in seawater by cathodic stripping voltammetry (CSV) were it not be for the coalescence of their responses in a single peak. Here, we modified the traditional CSV method of RSS analysis to allow individual recognition and quantification in thiol/thioamide mixes. Glutathione, cysteine, thiourea and thioacetamide in UV digested seawater were repeatedly analyzed shifting the deposition potential (E_{dep}) in the range +0.07 to −0.4 V at high resolution. The representation of peak height (i_p) and peak potential (E_p) vs E_{dep} resulted in different and distinctive profiles for each substance that allowed the selection of adequate E_{dep} ranges for their separate quantification. Copper saturation modified thiol profiles and cancelled the response of thioamides. The vs E_{dep} profiles explained the nature of the different thiols and thioamides present in the sample and permitted their individual quantification with excellent accuracy. The utility of the method was put to test with seawater modified with natural unknown RSS from pore waters and *Posidonia oceanica* exudates. Although both samples gave similar CSV signals, the vs E_{dep} profiles unveiled completely different electrochemical behaviors incompatible with a similar nature. Based on those profiles we hypothesized that pore waters released a glutathione/thiourea mix and that one or several unidentified RSS formed part of *P. oceanica* exudates. The analytical scheme proposed here opens a new door to the use of direct voltammetry in the qualitative and quantitative determination of RSS in natural waters.

1. Introduction

There is copious evidence that the speciation of copper and other trace metals in seawater is dominated by organic complexation [1–3]. The chemical and physical characteristics of the metal–ligand complexes modulate the scavenging [4,5], bioavailability [6] and solubility [7] of trace metals in seawater. Although the nature of those ligands remains unknown, previous works have suggested that thiols constitute the majority of the pool of copper ligands in natural waters [8–11].

Thiols are organics that include the sulfhydryl group (—SH) and play a paramount role in cell metabolism due to their detoxifying effect as metal ligands and reactive oxygen species scavengers [12]. Thiol sources to coastal waters include phytoplankton exudation [13], pore waters [14] or industrial and sewage effluents [11] suffering of quick degradation caused by photooxidation [15,16]. Thiols present a huge variety of forms: mercapto compounds, glutathione (GSH), cysteine, thioglycolic acid and many more, plus substitutions of the former (i.e., N-acetyl-L-cysteine), disulfur dimmers (i.e., oxidized glutathione, GSSG) and phytochelatins (GSH–cysteine chains) resulting in hundreds of possible compounds. Other reduced sulfur substances (RSS) of environmental relevance that could be found in seawater are: organosulfur compounds as thioamides (—CS—N<), dimethyl sulfide (DMS) and disulfide (DMDS), and a complex mix of inorganic compounds featuring sulfide, poly-sulfides and thiosulfate. Specifically, thioamides in equilibrium are ambidentate donors with both their S or N atoms available for coordination, which presence in natural waters is caused by their used in many fields of industry, agriculture and chemistry [17,18].

The high affinity of reduced sulfur for mercury facilitates the analysis of RSS by cathodic stripping voltammetry (CSV) using mercury electrodes [10,19–24]. RSS determination can also be performed by other analytical techniques after separation by high performance liquid chromatography [8,25] although, to our knowledge, no chromatographic technique has been developed to determine the concentration of thioamides in seawater. Analysis by CSV is direct, rapid, cheap and extremely sensitive, is not affected

* Corresponding author.
E-mail address: luis.laglera@uib.es (L.M. Laglera).

0039-9140/$ – see front matter © 2012 Elsevier B.V. All rights reserved.
doi:10.1016/j.talanta.2011.12.075

by low recoveries and does not require preconcentration or derivatization of unstable species (the case of many RSS). However, CSV is severely limited by coalescence, i.e., the merge in a single peak of the signals due to more than one compound. Up to date, chromatographic techniques have been required in the analysis of natural samples to separate their different RSS prior to their quantification.

Coalescence is the cause of another limitation: the selection of the model compound appropriate for internal calibration. Previous works selected the model RSS from a list of commercial reagents (sulfide, thiourea (TU), thioacetamide (TA), cysteine and GSH) which better overlapped the peak caused by the natural RSS [13,20,24,26,27]. The analytical routine was carried out setting the electrode at the unique deposition potential (E_{dep}) of maximum response for the model compound. This situation has translated in non-realistic procedures as the calibration of phytoplankton exudates with a compound of industrial origin (TA). Although voltammetry is used successfully to determine RSS that produce well-separated peaks [13,22,23], the only efforts put on the individual qualitative and qualitative analysis in seawater of RSS that produce overlapping CSV peaks have been by combined acidification/purge of the volatile fractions [22,24,28].

In this work, we propose the modification of the traditional CSV approach to measure RSS in seawater incorporating the use of multiple E_{dep}. We used two thiols (cysteine and GSH) and two thioamides (TA and TU) to show that the distribution of peak heights (i_p) and peak potentials (E_p) as a function of the E_{dep} used to deposit their Hg and Cu complexes gives distinctive individual profiles. Those profiles allowed the identification of appropriate E_{dep} ranges for their separate quantification in mixes. Copper additions proved useful to mask the contribution of thioamides. We used those profiles to obtain important information about the nature and concentration of RSS released into benthic chambers placed near the coast of the island of Cabrera (Spain).

2. Experimental

2.1. Instrumentation and reagents

All electrochemical measurements were obtained by a voltammeter (Autolab PGStat 10) connected to an electrode stand (Metrohm VA663) and controlled by the GPES 4.9 software (Eco Chemie BV). The cell consisted of a hanging mercury drop electrode (HMDE), a double junction reference electrode, Ag/AgCl, KCl (3 M), saturated AgCl, with a saltbridge filled with UV digested seawater and a glassy carbon rod as counter electrode. 10 mL samples were placed in a glass vessel and dearated with nitrogen before analysis.

Water used for reagent preparation was Milli-Q (MQ, Millipore). Ammonia (NH_4OH) (TraceSELECT Ultra, Sigma–Aldrich) was used from 1:1 dilutions in MQ water. Copper standard solutions were obtained from the dilution of an atomic absorption standard solution (Spectrosol, BDH) with MQ, and 0.1% 6 M HCl.

The pH buffer solution was 1 M boric acid (Suprapure, Merck) in MQ water with the addition of ammonia to fix the pH of the solution at 8.4 (NBS, National Bureau of Standards). A stock solution of 10 mM EDTA (Merck) was prepared in MQ water and NH_4OH at a pH of 8.3 to avoid pH drifting at increasing EDTA concentrations.

Standard solutions of thioacetamide, oxidized glutathione (GSSG), thiourea, sodium sulfide and thiosulfate (all from Sigma) were prepared freshly immediately before use by dissolution in MQ water in the presence of 0.01 M acetate buffer (pH ~4) and 50 μM EDTA to prevent oxidation [16]. Sodium sulfide and thiosulfate stock and standard solutions were also prepared in N_2 purged MQ water to determine if the decay (sulfide) or absence (thiosulfate) of the signal was due to the presence of oxygen in the solution with negative results.

Organic matter was removed from seawater by irradiation for 2 h in acid clean 30 mL quartz vessels with a 150 W high pressure mercury lamp placed into a quartz refrigerating jacket filled with distilled water.

2.2. Sample collection

Seawater samples were collected at Es Port de Cabrera (Cabrera; 39°08.745′N 02°56.123′E), Balearic Islands, Spain (Western Mediterranean) in summer 2009. Lush seagrass meadows of *Posidonia oceanica*, the predominant seagrass species in the Mediterranean meadows [29], covered the shallow sea bottom where 3 benthic chambers enclosing *P. oceanica* shoots and another 3 in sandy patch withing the meadows were deployed at 3 m water depth. The chambers consisted of a PVC cylinder (18 cm in diameter) with a sharpened side firmly inserted 7–10 cm into the sediments that held a polyethylene plastic bag with a sampling port (approximate volume 5 L). After a period of rest to allow the sedimentation of any resuspended material, bags were fitted to the cylinder and 100 mL was withdrawn immediately by means of 50 mL syringes that were carried to surface and their volume collected in LDPE bottles. The operation was repeated after 24 h. Seawater for UV digestion was collected close to the island of Cabrera by peristaltic pumping using Teflon tubing and online 0.2 μm filtering. All plastic material was previously cleaned by successive detergent and acid (HCl 30%) washing.

2.3. Determination of the concentration of thiols and thioamides in seawater

The procedure used here to determine the concentration of thiols, thioamides and natural RSS in seawater is based on previous CSV methods used for the determination of thiols in natural waters [10,27]. In those previous works, CSV scans of the natural sample in the presence of buffer were obtained at one unique E_{dep} corresponding to the potential of maximum response of a model compound. This model compound was selected as the commercial RSS that better overlapped the natural RSS peak. Subsequent calibration was performed by internal standard additions.

In this case, samples (10 mL) were buffered with a borate/ammonia solution for a concentration of 10^{-2} M (pH 8.4) and spiked with increasing additions of 100 μM EDTA until a stable peak was found (range 2–4 × 10^{-4} M EDTA). When masking of thioamides was required, a second 10 mL aliquot was spiked with borate buffer and 500 or 750 nM copper. Aliquots were placed in the electrochemical cell and after 300 s purge with N_2, RSS were deposited onto the HMDE for 60 s at no less than 12 different potentials in the range +0.07 to −0.4 V. The amplitude of the E_{dep} range was constrained by the oxidation of the mercury electrode and the beginning of the RSS peak. An E_{dep} of −0.1 V was used at the beginning and the end of the sequence to check the stability of the measurement. After 8 s quiescence, the potential was shifted from the E_{dep} to −0.8 V in square wave mode with the following parameters: frequency 10 Hz, pulse height 25 mV and step increment of 2.5 mV. The E_p of the CSV peaks of Hg–RSS and Cu–RSS complexes were located at potentials in the range −0.5 to −0.65 V (except for cysteine) depending on their nature and the copper/RSS ratio.

Internal calibrations were performed with those RSS that the visual inspection of the vs E_{dep} profiles marked as candidates to be present in the sample. Model RSS were spiked sequentially to the same volume. Analyses in the whole E_{dep} range were performed after every spike. Sensitivities were obtained at every E_{dep} from the peak increase forced by the addition of the model RSS. Concentrations were calculated using the peak heights obtained initially before additions. The novelty in this case was that the E_{dep} selected

was not that giving a maximum i_p but the E_{dep} where the signal was either, free of interferences from the rest of RSS targeted in this study, or those interferences could be subtracted from the i_p obtained found at other E_{dep}.

We tried here two different types of calibration. One traditional where a calibration curve was built from triplicates of i_p obtained for the sample and two internal additions of a model RSS at a characteristic E_{dep}: +0.07 V for TU (minus i_p (0 V)), −0.02 V for TA (minus i_p (−0.3 V)) and −0.3 V for GSH. The limits of detection (LOD) were calculated from 3 times the standard deviation of 5 consecutive measurements. Those are a function of the relative proportions of the constituents of the RSS mix.

The second calibration method was based on the possibility to obtain different sensitivities and concentrations at each E_{dep} and the possibility that after the addition of the model RSS the i_p vs E_{dep} profile could not mimic the previous profile when more than one RSS was present in solution. We proceeded with "multicalibrations" calculating first the sensitivity for every RSS at each E_{dep} from single measurements before and after model RSS addition. Using initial i_p, obtained before the beginning of the calibration, we reported RSS concentrations as the average and the standard deviation of the concentrations obtained in a continuous range of E_{dep} that gave coherent values. For mixes of known composition those ranges were +0.07 to +0.03 V for TU (subtracting i_p at E_{dep} = 0 V), 0 to −0.1 V for TA (subtracting i_p at E_{dep} = −0.3 V) and −0.25 to −0.4 for GSH. The number of data pairs used is given in between parenthesis (n = 1–14). The goal was to evaluate the robustness of the quantification via the reproducibility (from the standard deviation) of the determination in an E_{dep} range. The recording of triplicates at every E_{dep} for sample and standard additions would increment the statistical robustness but was discarded due to the excessive accumulation of mercury at the bottom of the cell and the long duration of the extended analysis (over 4 h per aliquot). A scheme summarizing the procedure is shown in Figure S1.

3. Results and discussion

3.1. Thiol and thioamide CSV signals and peak coalescence

The high affinity of reduced sulfur for soft acids is the cause of the pointed and sensitive signals that RSS exhibit by CSV. Sulfur binds to the mercury of the HMDE forming a film, and scanning to more negative potentials results in the reduction of the complex [30]. Complexes of some sulfur compounds with other metals as copper are also electrolabile [26,31,32]. The reduction potentials of some RSS on the HMDE are different enough to allow their individual quantification [23]. However, the CSV peaks of some RSS (sulfide, polysulfides, glutathione, thiourea and thioacetamide) of environmental relevance fall in a narrow potential interval [33] with the result of coalescence and the impossibility to quantify or even recognize their individual presence in natural samples. Changes in pH [23] or blowing out of sulfide and other volatile RSS by nitrogen purging [34] have been suggested to differentiate some of these fractions. In Fig. 1 we show how the vicinity of the CSV peaks of selected thiols and thioamides in the presence of EDTA makes impossible their simultaneous quantification except for the case of cysteine complexes that are reduced at more positive potentials. A ternary mix of GSH, TU and TA appeared as a single peak. EDTA additions increased the CSV peaks in thioamide solutions and in natural samples to a plateau and further decay at EDTA additions around and over 1 mM. The function of EDTA is to sequester copper (and other metals with the possibility to interfere) and permit the exclusive analysis of Hg–RSS complexes. This justifies its addition to all samples except those saturated with copper.

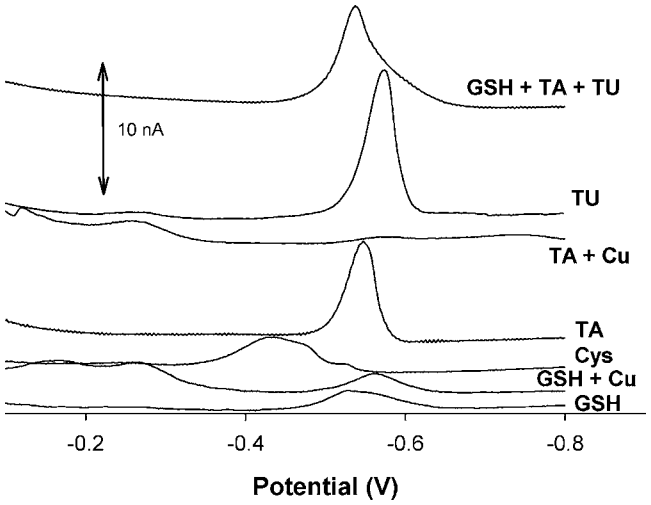

Fig. 1. CSV scans of 50 nM GSH, 50 nM GSH + 750 nM Cu, 30 nM cysteine, 20 nM TA, 30 nM TA + 100 nM Cu, 30 nM TU and a mix of 40 nM TA + 20 nM TA and 20 nM TU. Conditions: 10 mL UV digested seawater at pH 8.4, 300 μM EDTA (except for GSH/Cu and TA/Cu) and 60 s deposition at 0 V (except for TU, E_{dep} = +0.05 V).

Fig. 1 also shows that the E_p of GSH is a function of the copper concentration as thiol copper complexes show at more negative potentials than their mercury analogous [26,35]; the degree of peak coalescence of RSS mixes is as a result a function of copper/RSS ratios.

The method we present herein does not require changes of the psychochemical properties of the sample and permits the qualitative and quantitative analysis of mixes of GSH with thioamides. The method has the potential to be extended to the analysis of other RSS. The presence of mixes of thiols and thioamides in natural waters has been hypothesized before in waters of the Scheldt estuary [10]. This analytical routine could have confirmed or denied the hypothesis.

3.2. Effect of E_{dep} and copper concentration on the reduction peak of thiols and thioamides in seawater

Fig. 2 shows the dependence of E_p and i_p with respect to E_{dep} in the range +0.07 to −0.4 V for the CSV analysis of TU, TA, GSH, GSSG and cysteine in UV digested seawater at pH 8.4 in the presence of 300 μM EDTA. Fig. 2 also shows the same profiles when EDTA is substituted for 500 nM Cu to force the formation of Cu–RSS complexes. As a result, all RSS tested gave distinctive i_p vs E_{dep} and E_p vs E_{dep} profiles.

In the case of thioamides, peaks at E_{dep} close to the oxidation potential of mercury (∼+0.1 V) were much higher than those from similar concentrations of thiols in consonance with previous works [33]; however, peaks vanished sharply as E_{dep} moved to more negative potentials. The i_p vs E_{dep} profile of thioamides took the form of an inverted S (Fig. 2A) whereas their E_p vs E_{dep} profiles were S-shaped (Fig. 2C). TU became easily distinguishable from TA as their peaks vanished at E_{dep} < 0 and <−0.1 V respectively (Fig. 2A). Copper additions above 10^{-7} M removed the contribution of thioamides to CSV scans (Fig. 1).

Thiols also showed a distinctive behavior. The Hg–cysteine complex (Fig. 2A and C) showed a E_p vs E_{dep} profile nearly flat and a i_p vs E_{dep} profile with a peak decrease at E_{dep} < −0.2 V until the peak disappeared at $E_{dep} \sim E_p$ (∼−0.4 V). A 500 nM copper addition shifted the cysteine peak to more negative potentials by 80–120 mV and increased significantly the peaks without changing the shape of the i_p vs E_{dep} profile. However, the E_p vs E_{dep} profile of Cu–cysteine complexes took a distinctive inverted S-shape, opposite to the shape shown by Cu–thioamide complexes (Fig. 2C). As the E_p vs E_{dep}

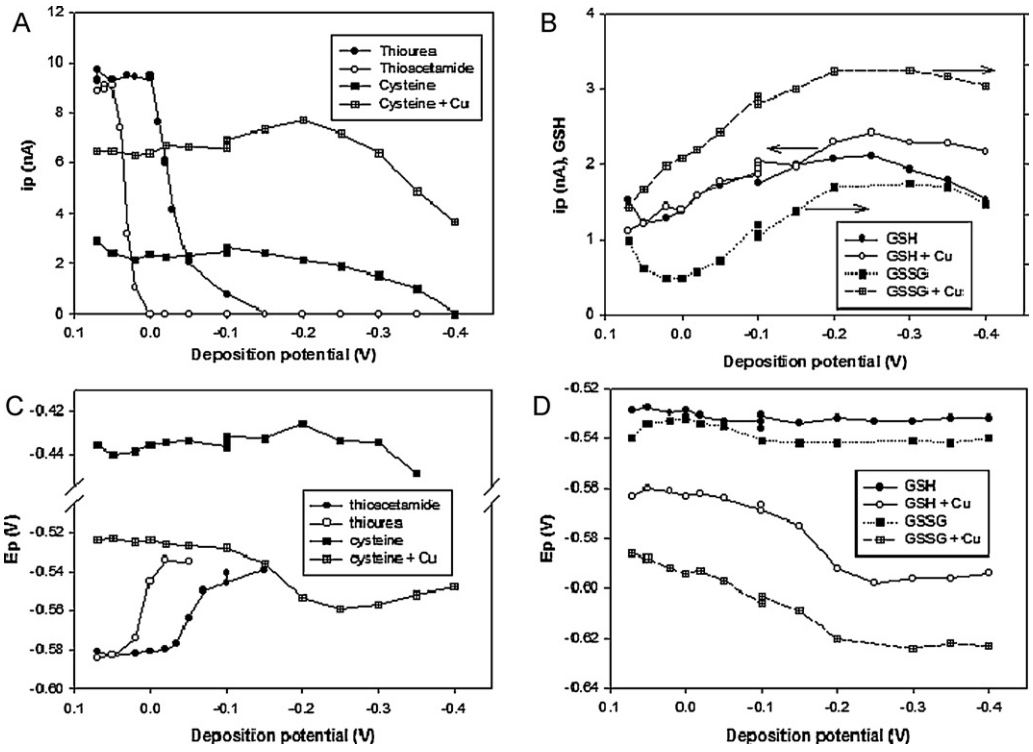

Fig. 2. The effect of the deposition potential on the peak height and peak potential of the CSV analysis of model thiols and thioamides in UV digested seawater at pH 8.4. The analyses were obtained in the presence of 300 μM EDTA and repeated in the presence of 500 nM Cu. (A) and (C): 20 nM thiourea, 20 nM thioacetamide and 30 nM L-cysteine, (B) and (D): 30 nM glutathione reduced and 60 nM glutathione oxidized. Thioamide peaks disappeared in the presence of copper.

profiles of GSH and GSSG also moved from flat to inverted S-shaped curves after copper addition (Fig. 2D), the change of the E_p vs E_{dep} profile after copper saturation is a powerful tool to recognize the presence of thiol groups in the sample. Sharp changes at potentials around −0.15 V are related to the redox state of the excess copper on the surface of the electrode; free copper is reduced at more positive potentials at the surface of the HMDE that becomes actually a copper-mercury amalgam [32]. GSH and GSSG mercury complexes showed identical i_p vs E_p profiles with a plateau in the range −0.2 to −0.4 V, a progressive reduction of the peak up to E_{dep} = 0 V, and slightly higher peaks at potentials close to the mercury oxidation potential. After copper addition, the i_p vs E_{dep} profiles remained the same except in the range +0.07–0 V where the decrease of the peak at intermediate E_{dep} continued (Fig. 1B). Whereas copper addition did not increase the GSH peak (Fig. 1B), the GSSG peak increased approximately 2-fold. Dimmers of cysteine [31] and glutathione [32] are reported to experiment disulfide bridge dissociation on the surface of HMDE during the accumulation step. Therefore, the increase of the GSSG peak after copper addition was not caused by Cu-triggered dissociation, but by changes of the copper/thiol ratio. This ratio also explains the significant increase of the cysteine peak after copper addition (3-fold) as cysteine is much more sensitive to this ratio than GSH [35].

We tried to reproduce this procedure for some inorganic RSS but it was not possible due to different causes: for sulfide, and according to previous works in seawater using CSV on the HMDE [19], we obtained a sulfide reduction peak at −0.58 V that rapidly decreased with consecutive analyses until stabilization at 2–5% of its initial value. The instability of the sulfide peak was assigned to high mercury concentrations in solution (from partial dissolution of the HMDE and the discarded mercury accumulated at the bottom of the voltammetric cell with analyses) combined with the very low solubility of HgS ($K_{sp} = 10^{-52.7}$ [36]). This has been confirmed by stable sulfide signals obtained when HMDE is coupled to a flow cell that removes the excess of dissolved Hg [19]. In the presence of 500 nM copper the stability of the sulfide peak did not improve and the peak at −0.58 V was replaced by a peak overlapping the copper peak at ∼−0.2 V that we did not investigate further. In the case of sulfite and thiosulfate we could not obtain a CSV peak in our experimental conditions although both are reported to give a reduction peak by CSV at pH 8 [23].

From Fig. 1 we can infer that copper addition becomes a valuable tool to remove the contribution of thioamides to the CSV signal and identify the presence of thiol compounds from the distinctive shift of the E_p vs E_{dep} profile from flat to an inverted S-shape.

From the results in Fig. 2 we can obtain the E_{dep} ranges where the individual compounds presented in this study could be determined when mixed. In the case of GSH, at E_{dep} more negative than −0.2 V, the CSV peak is free of any contribution from thioamides. At potentials in the range 0 to −0.15, the CSV peak is a signal overlapping the contributions of GSH and TA and at potentials in the range of +0.07 to +0.02 V, the three RSS coalesce in a single signal. This distribution justified the use of i_p (E_{dep} = −0.3 V) to determine GSH, i_p (E_{dep} = −0.02 V)–i_p (E_{dep} = −0.3 V) to determine TA and i_p (E_{dep} = +0.07 V)–i_p (E_{dep} = 0 V) to obtain the concentration of TU. The determination of cysteine can be carried out without the need to make use of this scheme because, in the presence of EDTA, is clearly separated from the rest of RSS, and after copper saturation, that moves the cysteine peak to ∼−0.6 V, thioamides are gone and glutathione has experienced a similar shift to the right that prevents overlapping

3.3. Qualitative and quantitative analysis of thiol/thioamide mixes in seawater in the presence of EDTA

Prior to the study of mixes of thiols and thioamides, the use of vs E_{dep} profiles was tested for the quantification of a binary mix of TU and TA (10 and 20 nM, respectively) in UV digested seawater in the

Table 1
Results obtained form the determination of thiols and thioamides mixes in UV digested seawater. All concentrations in nM. Standard internal calibrations at appropriate single E_{dep} and muticalibrations in E_{dep} ranges are compared. Peaks used for single E_{dep} calibrations: TU, i_p (E_{dep} = +0.07 V)–i_p (E_{dep} = 0 V); TA, i_p (E_{dep} = −0.02 V)–i_p (E_{dep} = −0.3 V); GSH, i_p (E_{dep} = −0.3 V). LOD from 3 times the standard deviation from 5 analyses. E_{dep} range calibration averaged peaks in the intervals: TU, (+0.07 to +0.03 V)–i_p (E_{dep} = 0 V); TA, (0 to −0.1 V)–i_p (E_{dep} = −0.3 V)); GSH (−0.2 to −0.4 V). n is the number of concentrations averaged at consecutive E_{dep}.

RSS mix	Calibration method	[GSH] (Recovery) LOD/n	[TU] (Recovery) LOD/n	[TA] (Recovery) LOD/n
20 nM TA/10 nM TU	Single E_{dep}	–	9.6 ± 1.3 (96%) 3.7	21.3 ± 0.7 (106%) 1.3
	E_{dep} range	–	12.5 ± 0.9 (125%) n = 3	21.2 ± 1.8 (106%) n = 9
40 nM GSH/20 nM TU/20 nM TA	Single E_{dep}	44.3 ± 2.0 (111%) 4.9	19.8 ± 1.1 (99%) 3.6	21.4 ± 1.0 (107%) 1.3
	E_{dep} range	43.0 ± 4.8 (108%) n = 8	18.3 ± 5.4 (92%) n = 5	18.9 ± 1.5 (94%) n = 5
40 nM GSH/25 nM TA	E_{dep} range	40.5 ± 10.9 (101%) n = 5	–	26.2 ± 4.8 (105%) n = 6
50 nM GSH/25 nM TA + 750 nM Cu	E_{dep} range	48.1 ± 1.2 (96%) n = 4	–	–

presence of 300 μM EDTA. The dependence of i_p and E_p vs E_{dep} is shown in Fig. 3 and corresponds to the accumulation of the features observed for isolated thioamides in Fig. 2: peaks were absent at E_{dep} < −0.15 V increasing abruptly at more positive potentials, and the E_p vs E_{dep} profile was close to an S-shape. The presence of more than one thioamide can be inferred from the presence of peaks at E_{dep} < 0 V (pointing to TA), and the increase of i_p and decrease of E_p in the E_{dep} range +0.07 to +0.02 V (pointing to a TU/TA mix). Those features were mimicked by successive additions of 20 nM TU and 20 nM TA (an extra addition of 20 nM TA and TU is not shown in Fig. 3). The results of quantifying TA (i_p (E_{dep} = −0.02 V)) and TU (as i_p (E_{dep} = +0.07 V)–i_p (E_{dep} = 0 V)) are shown in Table 1. Good recoveries of 96% for TU (sensitivity = 0.381 nA nM^{-1}, r^2 = 0.998) and 106% for TA (sensitivity = 0.277 nA nM^{-1}, r^2 = 0.999) were obtained. LOD calculated from 3× the standard deviation of 5 scan replicates of the TU/TA mix were found to be 3.7 nM and 1.3, respectively.

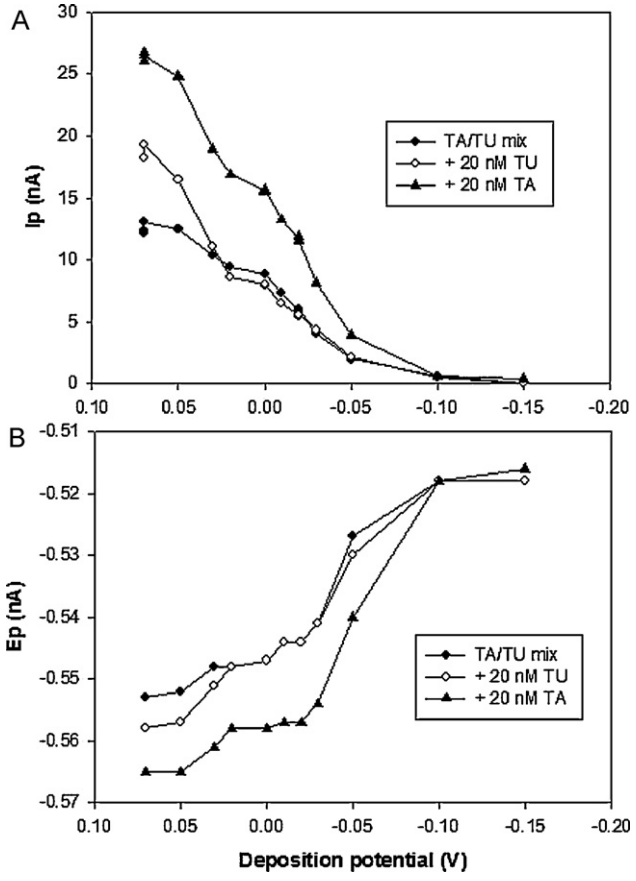

Fig. 3. The effect of the deposition potential on the peak height (A) and peak potential (B) for the CSV analysis of 10 mL UV digested seawater at pH 8.4 in the presence of 300 μM EDTA, 10 nM TU and 20 nM TA. The effect of the sequential addition of 20 nM TU and 20 nM TA for calibration purposes is also shown.

Because more than one E_{dep} can be used we tested the multicalibration method at the characteristic E_{dep} ranges described in the experimental section. The method offered a good estimate of both the TU and TA concentrations with recoveries of 125% and 106%, respectively (Table 1).

Next, we checked the suitability of the method in the worst case scenario of a ternary mix. A 10 mL volume of buffered UV digested seawater was spiked with 300 μM EDTA, 40 nM GSH, 20 nM TA and 20 nM TU. The contributions of the three RSS coalesced in a single peak in the whole E_{dep} range of the study (see Fig. 1). Calibration was performed via successive additions of 2 × 40 nM GSH (using i_p (E_{dep} = −0.3 V)), 2 × 20 nM TU (using i_p (E_{dep} = +0.07 V)–i_p (E_{dep} = 0 V)) and 2 × 20 nM TA (using i_p (E_{dep} = −0.02 V)–i_p (E_{dep} = −0.3 V)) to the same volume. The effect of every second RSS addition on i_p and E_p is shown in Fig. 4A and B and the concentrations and recoveries are shown in Table 1. As for the TU/TA mix, the recoveries obtained for the three RSS were excellent: 111% GSH, 99% TU and 107% TA. The three calibrations gave the following parameters: GSH (sensitivity = 0.031 nA nM^{-1}, r^2 = 0.999), TU (sensitivity = 0.553 nA nM^{-1}, r^2 = 0.999), TA (sensitivity = 0.376 nA nM^{-1}, r^2 = 0.999) (curves can be seen in Figure S1). The LOD (n = 5) were also found low, being respectively 4.3 nM (GSH), 3.6 nM (TU) and 1.3 nM (TA) despite the complexity of the mix. For GSH, concentrations in coastal waters have been reported in the range 0–40 nM [11,14,37] which underlines the worth of the method. Because linear behaviors have been reported up to 5 min for the CSV analysis of GSH in seawater [26], the method is susceptible to be used for subnanomolar concentrations.

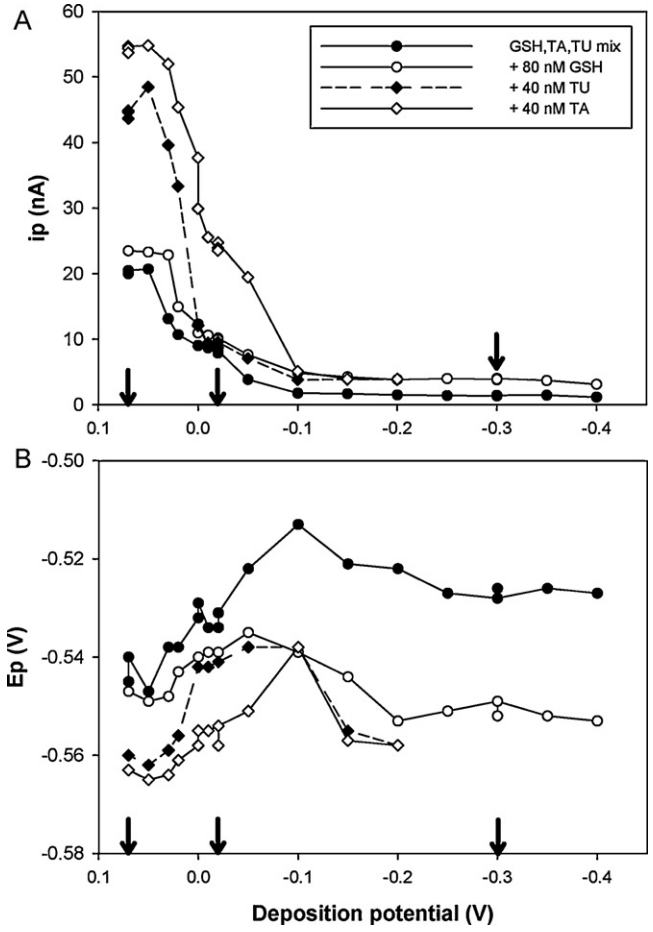

Fig. 4. The effect of the deposition potential on the peak height (A) and peak potential (B) for the CSV analysis of 10 mL UV digested seawater at pH 8.4 in the presence of 300 μM EDTA, 40 nM GSH, 20 nM TU and 20 nM TA. The effect of the sequential addition of 80 nM GSH, 40 nM TU and 40 nM TA for calibration purposes is also shown. Arrows indicate the deposition potentials selected for the determination (from left to right) of TU, TA and GSH.

Table 1 also presents the excellent recoveries found using multicalibration: 92%, 94% and 108% for TU, TA and GSH respectively. Although the multicalibration method is prone to give higher standard deviation coming from the combination of analyses in different conditions and the absence of replicates at each E_{dep}, in samples containing unknown mixes of RSS can give a better estimation of the validity of the method. This is due to the huge error added to the calculation when a model RSS producing a different i_p vs E_{dep} profile is added to the solution for calibration. The initial i_p vs E_{dep} profile would be modified and the sensibilities calculated would not correspond to that of the original compound, poisoning the determination of concentrations. To reduce the uncertainty, replicates at every E_{dep} could be performed but they would extend the duration of the analysis from 1–2.5 h to 4–7 h (actual time is a function of the number of RSS that have to be used for sequential calibration).

3.4. Quantitative analysis of a thiol/thioamide mix in seawater in the presence of excess Cu

According to results found for TU and TA (Fig. 1), RSS saturation with copper should free CSV scans from any contribution due to thioamides. To test this hypothesis we proceeded to compare the accuracy of the quantification of a GSH/TA mix in UV digested seawater with and without copper saturation. Multicalibrations were performed in the whole E_{dep} range +0.07 to −0.4 V to track interferences at specific E_{dep}.

Table 1 shows the results from the analysis of 40 nM GSH and 25 nM TA in UV digested seawater in the presence of 300 μM EDTA and from its calibration by sequential additions of 20 nM TA and 50 nM GSH. Multicalibration in the E_{dep} ranges appropriate for GSH and TA gave again excellent recoveries of 101% for GSH (E_{dep} range: −0.2 to −0.4 V; $n = 5$) and 105% for TA (E_{dep} range +0.07 to −0.02 V; $n = 6$).

Next, we tried the quantification of GSH in a 50 nM GSH and 25 nM TA mix in the presence of 750 nM copper using multicalibration after addition of 80 nM GSH (results in Fig. 5). In agreement with the results shown in Fig. 2, the addition of copper diminished the peaks obtained at positive E_{dep} (due to the electroinactivity of Cu–TA complexes) and shifted them to more negative potentials due to the replacement of Hg-GSH complexes for Cu–GSH complexes (Fig. 5A). According to the effects predicted using the profiles shown in Fig. 2, copper saturation moved the E_p vs E_{dep} profile from a S-shape to an inverted S-shape, and the i_p vs E_{dep} profile changed from a S-shape to a domed shape (Figs. 4 and 5). This is the transition expected from thioamide-dominated profiles to those characteristic of copper–thiol complexes and proved the possibilities of the vs E_{dep} profiles before and after copper saturation for the identification of the RSS present in the sample.

The addition of 80 nM GSH replicated the domed shape of i_p vs E_{dep} profile in the whole E_{dep}. The preservation of the i_p and E_p vs E_{dep} profiles after the addition of a model RSS is a more robust proof of the nature of the natural RSS than the traditional similarity of sample and model E_p. The suppression of the contribution of TA should have allowed the accurate determination of the GSH concentration in the whole E_{dep} range. However, this was not the case and at $E_{dep} > -0.2$, GSH concentrations were severely underestimated (Fig. 5C). In order to precise the cause of this effect we made an extra spike of 40 nM TA. The effect is shown in Fig. 5B and C and proved that Cu–TA complexes, despite their nonlability, interfered with the analysis of GSH forcing a small peak decrease at $E_{dep} > -0.2$ V. In the presence of TA and excess copper, GSH can only be accurately resolved at $E_{dep} < -0.2$ V. We did not investigate further whether the nature of the interference was due to electrode surface processes or competition for copper in between ligands. Once this effect is taken into consideration, we obtained from the determination in the E_{dep} range −0.4 to −0.25 V an excellent recovery of 96% (Table 1).

3.5. Application to the analysis of environmental samples

Analysis based in vs E_{dep} profiles was used in natural samples collected from benthic chambers in contact with either sandy coastal bottom or *P. oceanica*. Seawater withdrawn immediately after chamber closure ($t = 0$) presented a small CSV peak (0.3–0.6 nA) at −0.52 V due to the necessity for divers to fill the bags in situ with seawater modified by the influence of the surrounding sediment and/or plants. The strong increase of the CSV peak after 24 h equilibrium (2–3, up to 11 nA, see Fig. 6) indicated that RSS had been released. Fig. 6A shows an example of scans obtained from the CSV analysis of both types of samples after 24 h accumulation in the presence of 300 μM EDTA. Both scans show identical features with a sharp single peak of comparable magnitude at the same potential (−0.53 V), potential that would fit with three of the model RSS presented in Fig. 2 (TA, TU, GSH). For an initial estimation, we followed the traditional approach [13,20,27,35] to search for a model compound and found that GSH gave an overlapping peak ($E_{dep} = -0.1$ V). Used as model compound for calibration, we determined increments of the GSH concentration of 70 nM for the sandy bottom sample and 100 nM for the *P. oceanica* sample.

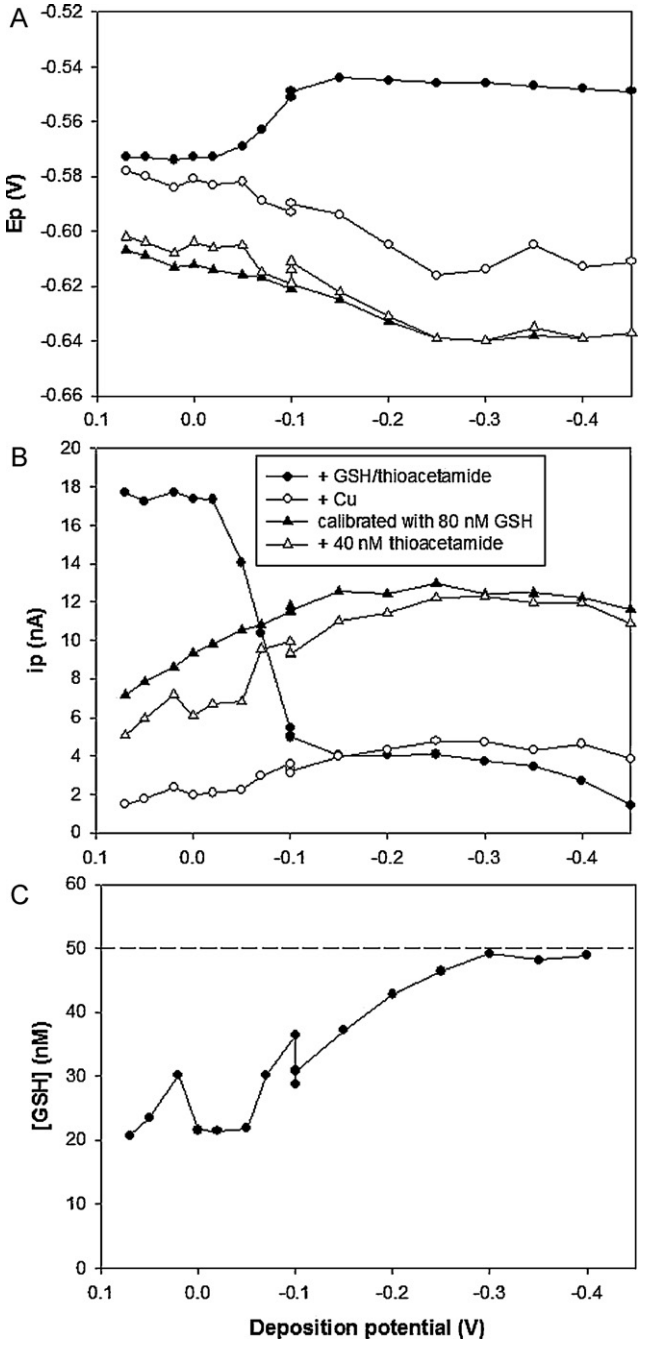

Fig. 5. The effect of the deposition potential on the peak potential (A) and peak height (B) for the CSV analysis of 10 mL UV digested seawater at pH 8.4 spiked with 50 nM GSH, and 25 nM TA before and after the addition of 750 nM copper. The effect of the sequential addition of 80 nM GSH for calibration purposes and 40 nM TA to study possible interferences is also shown. (C) The effect of deposition potential on the determination of the concentration of GSH from peak heights in (B).

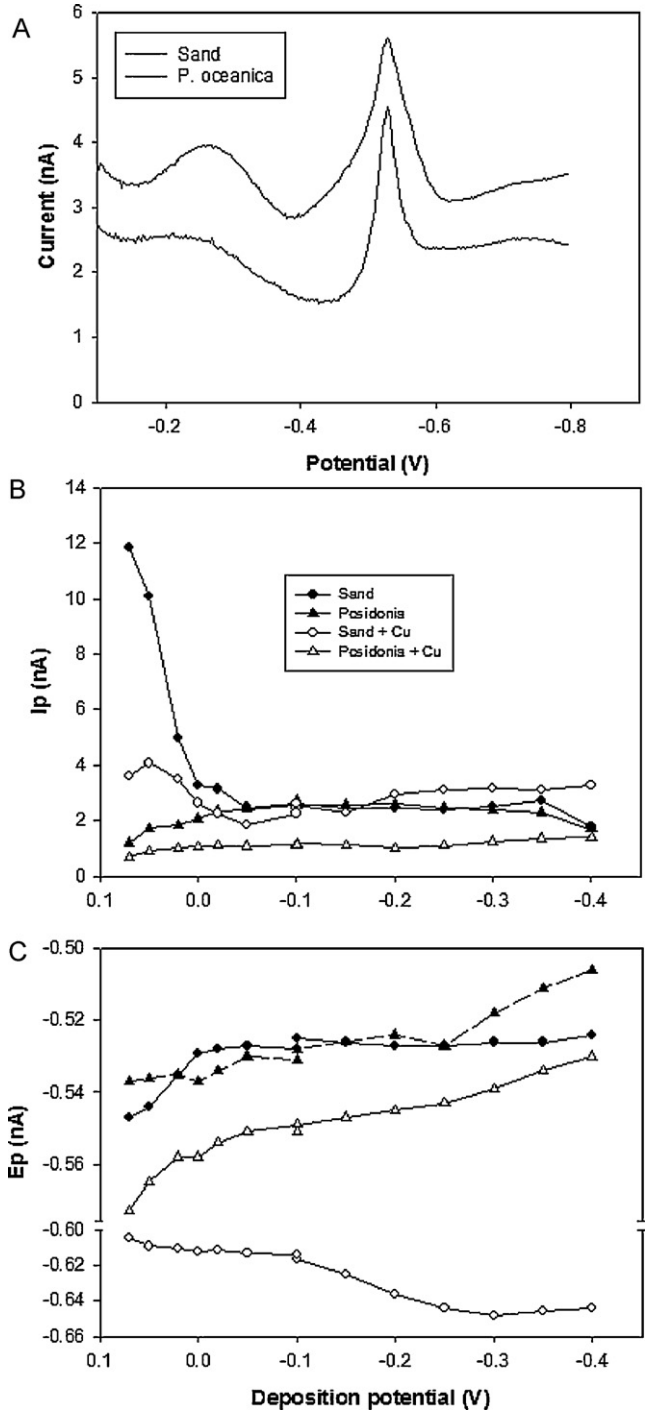

Fig. 6. (A) CSV scans of seawater collected from two benthic chambers after 24 h in contact with coastal sediment (sand) and with *Posidonia oceanica* shoots (*P. oceanica*). Conditions: 10 mL seawater at pH 8.4 in the presence of 300 μM EDTA, 60 s deposition at 0 V. (B) The effect of the deposition potential on the peak height of the analysis of the samples described in (A) and the same analysis replacing the EDTA with 500 nM copper. (C) For the same samples the effect of the deposition potential on the peak potential.

However, the use of the i_p and E_p vs E_{dep} profiles allowed a more complex interpretation (Fig. 6B and C). In the presence of EDTA, pore water exudates generated an inverted S-shaped i_p vs E_{dep} profile that in conjunction with a S-shaped E_p vs E_{dep} profile points to the presence of a thioamide in the sample. The sharp increase of peak heights and potentials found in the E_{dep} interval +0.05–0 V suggests that its nature is TU (Fig. 2A and C). Moreover, the presence of a well-defined peak at $E_{dep} > -0.1$ V, coupled to the shift of the RSS peak to more negative potentials after copper saturation, indicates that a second RSS is present, probably of thiol nature. The presence of a thioamide/thiol mix was backed further by the two effects caused by the addition of 500 nM Cu: a strong decrease of the peak at $E_{dep} > 0$ and change of the E_p vs E_{dep} profile to the inverted S-shape characteristic of thiol compounds. If we hypothesize that the whole RSS peak is caused by a mix of TU and GSH, we can use the multicalibration method to obtain their concentrations in the appropriate E_{dep} ranges: 10.0 ± 1.6 nM ($n = 3$) TU units in the E_{dep} range +0.07 to +0.02 V from the EDTA aliquot and 44.4 ± 2.6 nM

($n=9$) glutathione units in the E_{dep} range −0.4 to −0.1 V addition of 180 nM from the +Cu aliquot (calibrations as a function of E_{dep} in Figure S2).

The CSV analysis of *P. oceanica* exudates produced completely different features despite the similarity of the scans. The aliquot spiked with EDTA showed a dome-shaped i_p vs E_{dep} profile (Fig. 6B) that is close to the profiles recorded for cysteine and glutathione (Fig. 2A and B) suggesting the presence of a thiol. The E_p vs E_{dep} profile was approximately flat in agreement with the GSH profile shown before, except for a shift of E_p to slightly more positive potentials at $E_{dep} < -0.3$ V. Both vs E_{dep} profiles are incompatible with any significant presence of thioamides (Fig. 2A). However, results from the copper saturated aliquot show that the assignation of the CSV peak exclusively to GSH could be erroneous. The addition of 500 nM Cu caused: a reduction of the RSS peak of approximately 50% in the whole E_{dep} range and a displacement of ~20 mV to more negative potentials, shift much shorter than that caused to GSH in UV digested seawater (Fig. 2D). On the other hand, the addition of copper did not affect the flat E_p vs E_{dep} profile (thiols, if present, should have caused a change to an inverted S-shape). Additions of GSH to the copper aliquot provoked a change of the E_p vs E_{dep} profile to that characteristic of thiols, proving that GSH could not be the main component of the RSS peak (see Figure S3). Unfortunately, we could not find the compound or mix that fits the electrochemical behavior of *P. oceanica* exudates impeding the qualitative analysis of the sample and its proper calibration. Nevertheless, in order to have a rough estimation of the RSS concentration, we carried out a muticalibration with GSH in both aliquots with the following results: 98.5 ± 9.9 nM ($n=8$) GSH units in the wide E_{dep} range 0 to −0.35 V from the EDTA aliquot and of 19.7 ± 2.4 nM ($n=12$) GSH units in the whole E_{dep} range (−0.4 to +0.07 V) from the Cu aliquot (Figure S3). This last concentration was 80% short of the concentration found in the presence of EDTA. We hypothesize that the disparity is caused by the presence of more than one RSS of unknown nature that produce an overlapping signal. The copper complex of one of those RSS would be electrolabile and not the other, explaining the peak reduction after copper addition. Despite the uncertainty, the use of E_{dep} profiles was useful at least to detect that the nature of the RSS exudated by *P. oceanica* could not be assigned to GSH or thioamides as it would have been the case with the traditional CSV approach.

In a previous work, a peak of similar characteristics was found in seawater after incubation with dimethylsulfoniopropionate of several phytoplanktonic species to force an increase of its metabolic transformation to other sulfur compounds [24]. The peak produced by the fresh exudates could not be ascribed to elemental sulfur (as was present after copper addition) and other volatile RSS as sulfide (as the peak remained after a treatment of combined purge/acidification followed by neutralization). A similar RSS peak has been recently found in samples from a eutrophic marine lake [28]. However, the dependence of the signal as a function of E_{dep} was not studied.

GSH and TA have been used before for calibration of the concentration of exudates released from plants [27]. From our results, we hypothesize that RSS peaks by CSV detected in estuarine waters and algae cultures could have been calibrated with the wrong model compounds (usually GSH due to its good peak overlapping and biological origin). As a consequence, GSH role and presence in natural waters could have been overestimated [26] underlining the importance of the analytical approach presented here when chromatographic separation is not available.

4. Conclusions

We propose here an analytical scheme for the quantitative analysis of thiol and thioamide mixes in seawater based on the repetition of CSV measurements in the E_{dep} range +0.07 to −0.4 V of two sample aliquots spiked with EDTA (to maximize the RSS peak) and copper (to remove the contribution of thioamides), respectively. The model compound for calibration can be selected after visual inspection of the shape of the i_p vs E_{dep} and E_p vs E_{dep} profiles obtained in both aliquots. The method proved successful in quantifying binary and ternary mixes of TU, TA and GSH in seawater despite peak coalescence. Future work includes the preparation of a comprehensive database of i_p vs E_{dep} and E_p vs E_{dep} profiles of mercury and copper complexes of the many RSS can be found in seawater product of biota metabolism and anthropogenic activities.

The analysis of two natural samples reveal that underneath the simplicity of the RSS peak found lies a complexity that was ignored in previous uses of voltammetry.

The utility of the vs E_{dep} profiles could be easily extended adding the effect of other variables as pH or the addition of other trace metals. This could eventually lead to the use of direct voltammetry as an efficient tool for the analysis in seawater of individual RSS and complement chromatographic techniques.

Acknowledgments

This work was supported by the CABIARCA and EDASE projects (MARM, Ref: 27/2007; MICINN, Ref: CGL2008-00047/BTE) and by the "Conselleria d'Innovació, Interior i Justícia", Government of the Balearic Islands (project AAEE083/09). LML was supported by a Ramon y Cajal (MICINN) fellowship. We are grateful for the assistance with sample collection to Ana Massanet, Nuria Marbà and Pablo Vidal. We thank two anonymous reviewers for their assistance to improve the quality of the initial manuscript.

Appendix A. Supplementary data

Supplementary data associated with this article can be found, in the online version, at doi:10.1016/j.talanta.2011.12.075.

References

[1] K.H. Coale, K.W. Bruland, Limnology and Oceanography 33 (1988) 1084–1101.
[2] J.W. Moffett, R.G. Zika, L.E. Brand, Deep-Sea Research Part A: Oceanographic Research Papers 37 (1990) 27–36.
[3] C.M.G. van den Berg, Marine Chemistry 15 (1984) 1–18.
[4] L.S. Balistrieri, P.G. Brewer, J.W. Murray, Deep-Sea Research 28A (1981) 101–121.
[5] K. Hirose, Marine Chemistry 28 (1990) 267–274.
[6] W.G. Sunda, R.R.L. Guillard, Journal of Marine Research 34 (1976) 511–529.
[7] X.W. Liu, F.J. Millero, Marine Chemistry 77 (2002) 43–54.
[8] C.L. Dupont, J.W. Moffett, R.R. Bidigare, B.A. Ahner, Deep-Sea Research Part I: Oceanographic Research Papers 53 (2006) 1961–1974.
[9] M.F.C. Leal, C.M.G. van den Berg, Aquatic Geochemistry 4 (1998) 49–75.
[10] L.M. Laglera, C.M.G. van den Berg, Marine Chemistry 82 (2003) 71–89.
[11] C.L. Dryden, A.S. Gordon, J.R. Donat, Marine Chemistry 103 (2007) 276–288.
[12] A. Meister, in: D. Dolphin, O. Avramovic, R. Poulson (Eds.), Glutathione, Chemical, Biochemical and Medical Aspects. Part A, Wiley Interscience, New York, 1989, pp. 1–48.
[13] M.T.S.D. Vasconcelos, M.F.C. Leal, C.M.G. van den Berg, Marine Chemistry 77 (2002) 187–210.
[14] J.Z. Zhang, F.Y. Wang, J.D. House, B. Page, Limnology and Oceanography 49 (2004) 2276–2286.
[15] L.M. Laglera, C.M.G. van den Berg, Marine Chemistry 101 (2006) 130–140.
[16] M. Moingt, M. Bressac, D. Belanger, M. Amyot, Chemosphere 80 (2010) 1314–1320.
[17] T. Pérez-Ruiz, C. Martínez-Lozano, V. Tomás, R. Casajús, Talanta 42 (1995) 391–394.
[18] S. Abbasi, K. Khodarahmiyan, A. Farmany, Electroanalysis 23 (2011) 2386–2391.
[19] R. Al-Farawati, C.M.G. van den Berg, Marine Chemistry 57 (1997) 277–286.
[20] R. Al-Farawati, C.M.G. van den Berg, Environmental Science & Technology 35 (2001) 1902–1911.
[21] G.W. Luther III, E. Tsamakis, Marine Chemistry 27 (1989) 165–177.
[22] T.F. Rozan, S.M. Theberge, G.W. Luther III, Analytica Chimica Acta 415 (2000) 175–184.
[23] K.J. Umiker, M.J. Morra, I.F. Cheng, Microchemical Journal 73 (2002) 287–297.
[24] I. Ciglenecki, B. Cosovic, Marine Chemistry 52 (1996) 87–97.

[25] M.A. Dikunets, A.I. Elefterov, O.A. Shpigun, Analytical Letters 37 (2004) 2411–2426.
[26] A.-C. Le Gall, C.M.G. van den Berg, Analyst 118 (1993) 1411–1415.
[27] M.F.C. Leal, M.T.S.D. Vasconcelos, C.M.G. van den Berg, Limnology and Oceanography 44 (1999) 1750–1762.
[28] M. Plavšić, I. Ciglenečki, S. Strmečki, E. Bura-Nakić, Estuarine Coastal and Shelf Science 92 (2011) 277–285.
[29] N. Marba, C.M. Duarte, M. Holmer, M.L. Calleja, E. Alvarez, E. Diaz-Almela, N. Garcias-Bonet, Estuarine Coastal and Shelf Science 76 (2008) 710–713.
[30] T.M. Florence, Journal of Electroanalytical Chemistry 97 (1979) 219–236.
[31] U. Forsman, Journal of Electroanalytical Chemistry 122 (1981) 215–231.
[32] U. Forsman, Analytica Chimica Acta 166 (1985) 141–151.
[33] V. Stará, M. Kopanica, Analytica Chimica Acta 159 (1984) 105–110.
[34] F.Y. Wang, A. Tessier, J. Buffle, Limnology and Oceanography 43 (1998) 1353–1361.
[35] C.M.G. Vandenberg, B.C. Househam, J.P. Riley, Journal of Electroanalytical Chemistry 239 (1988) 137–148.
[36] A.E. Martell, R.M. Smith, Critical Stability Constants, Plenum Press, New York, 1977.
[37] H. Hu, S.E. Mylon, G. Benoit, Limnology and Oceanography 51 (2006) 2763–2774.